Supplementary Information

Green Synthesized Cu_2O-$Cu(OH)_2$@Cu Mesh Composites with Fenton-Like Catalytic Properties for the Degradation of Cationic and Anionic Dyes

Hala A. Al-Jawhari [1,*], and Nuha A. Alhebshi [1]

1 Department of Physics, King Abdulaziz University, Jeddah 21589, Saudi Arabia

* Correspondence: haljawhari@kau.edu.sa

1. *Supplementary Information*

Supposed Mechanism of Spinach Extract:

It has been reported that the rate of copper oxidation under humid conditions can be accelerated significantly in presence of alkali solutions [21, 22]. In such process Cu^{2+} ions are released constantly from the Cu substance into the alkali solutions whereas the naturally dissolved O_2 is reduced. Spinach is known as one of the alkaline powerhouse that has pH level of 6.6 -7.2 when cooked

We presume that the growth mechanism of Cu_2O from Cu particles in the alkaline spinach solution can be described with the same steps presented in [21].

The O_2 in air is dissolved in the solution and then adsorbed on the surface of Cu particles. This O_2 adsorption will oxidize the Cu atoms to Cu^{2+} ions as the following:

$$2Cu + O_2 + 2H_2O \rightarrow 2Cu^{2+} + 4OH^- \quad \textbf{Eq.1}$$

Through a very short time the Cu^{2+} ions can be captured through the coordination with OH^- to form $Cu(OH)_2$ according to the reaction;

$$Cu^{2+} + 2OH^- \rightarrow Cu(OH)_2 \quad \textbf{Eq.2}$$

Consequently, $Cu(OH)_2$ can be transformed to monoclinic CuO at low temperature of 60°C, following this reaction;

$$Cu(OH)_2 \rightarrow CuO + H_2O \quad \textbf{Eq.3}$$

In the presence of a reductant (such as glycerol in our case), the final compounds could be Cu_2O and glyceric acid according to the following equation:

$$2Cu(OH)_2 + O_2 + C_3H_8O_3 \rightarrow Cu_2O + C_2H_5O_2\text{-}COOH + 2OH^- + 2H_2O \quad \textbf{Eq.4}$$

2. *Supplementary Tables*

Table S1. Peak centers and peak areas of the Cu 2p for Cu M@200 and SG-Cu M@200 samples

Peak Parameters	**Cu M@200**		**SG-Cu M@200**	
	Cu $2p_{3/2}$	Cu $2p_{1/2}$	Cu $2p_{3/2}$	Cu $2p_{1/2}$
Peak Center of Cu^{+} in Cu_2O	932.4 eV	952.4 eV	932.5 eV	952.4-5 eV
Peak Center of Cu^{2+} in CuO	933.7 eV	953.7 eV	----	----
Peak Center of Cu^{2+} in $Cu(OH)_2$	935.0 eV	955.0 eV	934.5 eV	954.5 eV
Peak Area of Cu^{+} in Cu_2O	4000 a.u.	1790 a.u.	900	400
Peak Area of Cu^{2+} in CuO	4000 a.u.	1790 a.u.	0	0
Peak Area of Cu^{2+} in $Cu(OH)_2$	2000 a.u.	895 a.u.	1800	800
Area Ratios of Cu^{+} : Cu^{2+} : Cu^{2+} in Cu_2O : CuO : $Cu(OH)_2$	2 : 2 : 1	2 : 2 : 1	1 : 0 : 2	1 : 0 : 2

Table S2. Peak centers and peak areas of O 1s for Cu M@200 and SG-Cu M@200 samples

Peak Parameters	**Cu M@200**	**SG-Cu M@200**
	O 1s	O 1s
Center of O^{2-} in Cu_2O	530.8 eV	530.8 eV
Center of O^{2-} in CuO	529.8 eV	----
Center of O-surf. in $Cu(OH)_2$	531.9 eV	531.9 eV
Center of O-surf. in $Cu(OH)_2$	533.4 eV	533.4 eV
Area of O^{2-} in Cu_2O	1000 a.u.	1000 a.u.
Area of O^{2-} in CuO	2078 a.u.	0
Area of O-surf. in $Cu(OH)_2$	2006 a.u.	5030
Area of O-surf. in H_2O	1678 a.u.	1622 a.u.
Area Ratios in Cu_2O : CuO : $Cu(OH)_2$	1 : 2 : 2	1 : 0 : 5

Table. S3 Brief comparison between our results and other reported Cu_xO@Cu composites

Catalyst	Form	Preparation Temp /time	dye	Light	Intensity (mW/cm^2)	Degrad. %	Rate $m.min^{-1}$	Time (min)	year	Ref.
Cu_2O-$Cu(OH)_2$@Cu	Mesh	Green synthesis **200°C /1 hr**	**MB**	Natural sun light	**5**	**89.4%**	**94.5**	**90**	**This work**	
			MO			**93%**	**126.5**	**40**		
CuxO@Cu + H_2O_2	Mesh	Green synthesis 300°C /1 hr	MB	Natural sun light	7	100%	63.2	60	2020	[14]
CuxO@Cu	Mesh	Green synthesis 300°C /1 hr	MB	Natural sun light	7	52%	9	120	2020	[14]
Cu/Cu_2O	Film	Green synthesis 200°C /0.5 hr	MB	Natural sun light	3	97.7%	20	180	2019	[13]
Cu/Cu_2O/CuO	Mesh	Thermal oxidation **500°C / 9 h**	RhB	Visible (lamp)	13.8	72 %	12	120	2017	[34]
Cu/CuO + H_2O_2	Film	Sputtered @ RT + chemical reduction	MB	Visible (lamp)	50	100%	40	120	2017	[35]
Cu/Cu_2O	Powder	Green synthesis **400°C /2 h**	MB	Visible (lamp)	50	99 %	-	150	2017	[36]
Cu-CuO + H_2O_2	Powder	Chemical microreactor	MB	**UV**	-	98.5%	109	50	2017	[37]
CuO/Cu_2O NWs	powder	Chemical method 40◦C for 6 h	MO	Visible (lamp)	**150**	100%	-	30	2017	[38]

3. *Supplementary Figures*

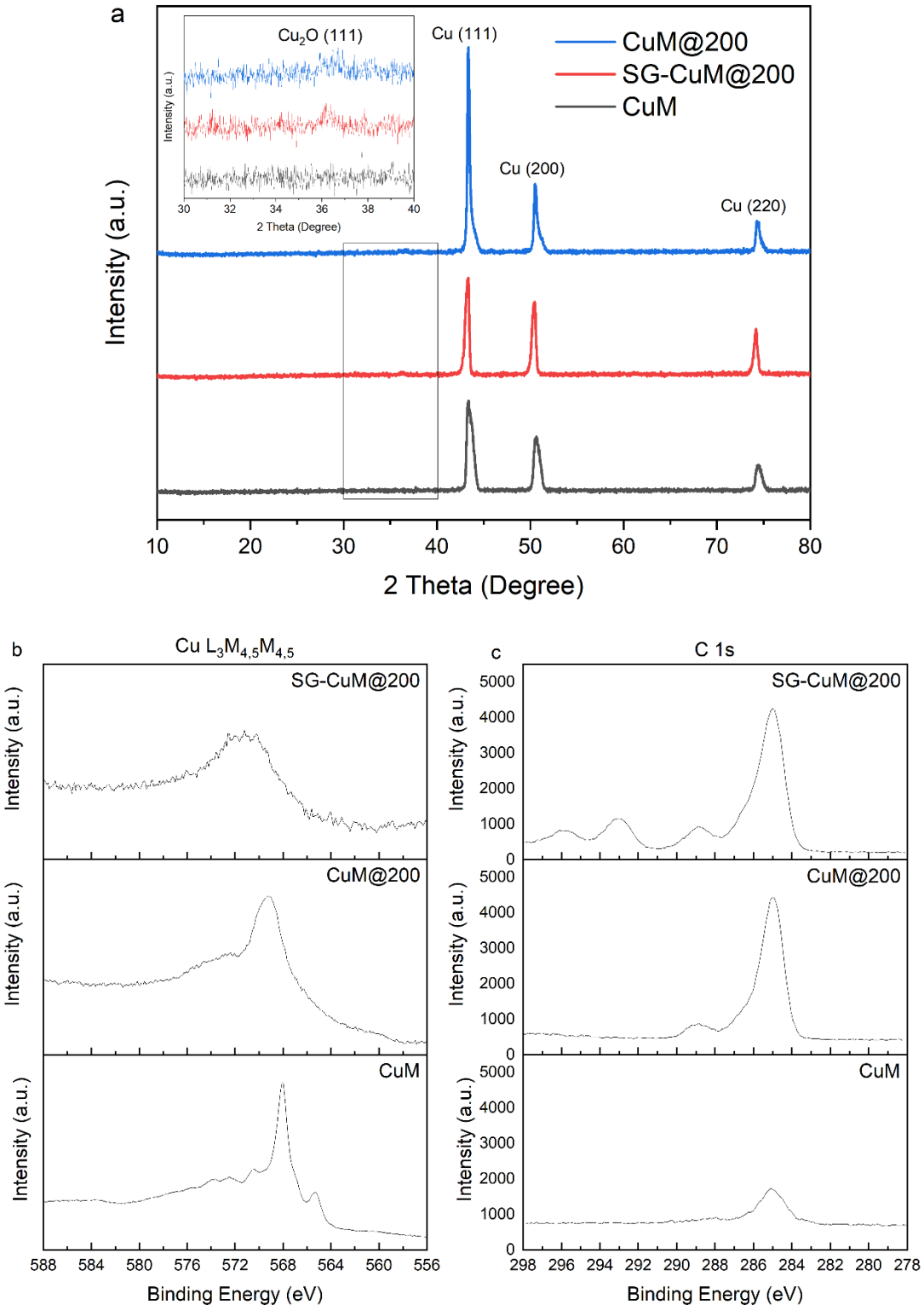

Figure S1. (a) XRD spectra, (b) XPS spectra of Cu $L_3M_{4,5}M_{4,5}$ and (c) XPS spectra of C 1s core peaks for as-prepared CuM, CuM@200 and SG-CuM@200 samples

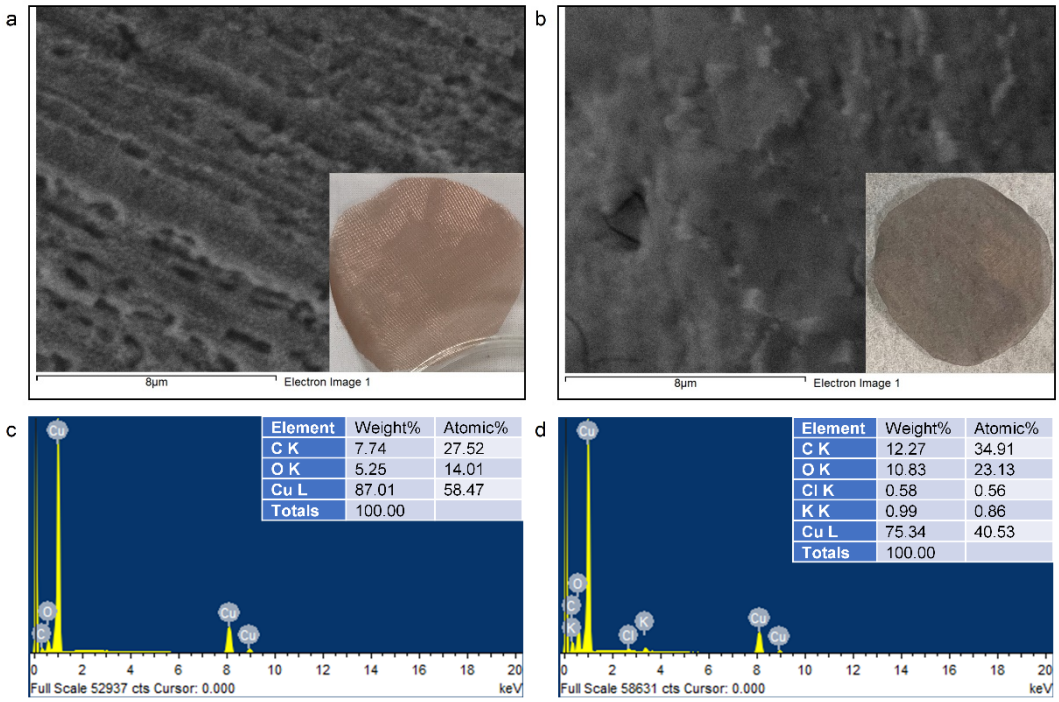

Figure S2. (a and b) SEM images of the as-prepared CuM and SG-CuM@200 samples, respectively, with photographs of the samples in the insets and (c and d) EDS spectra of both samples, respectively, with tables of the elemental and atomic weight percentages

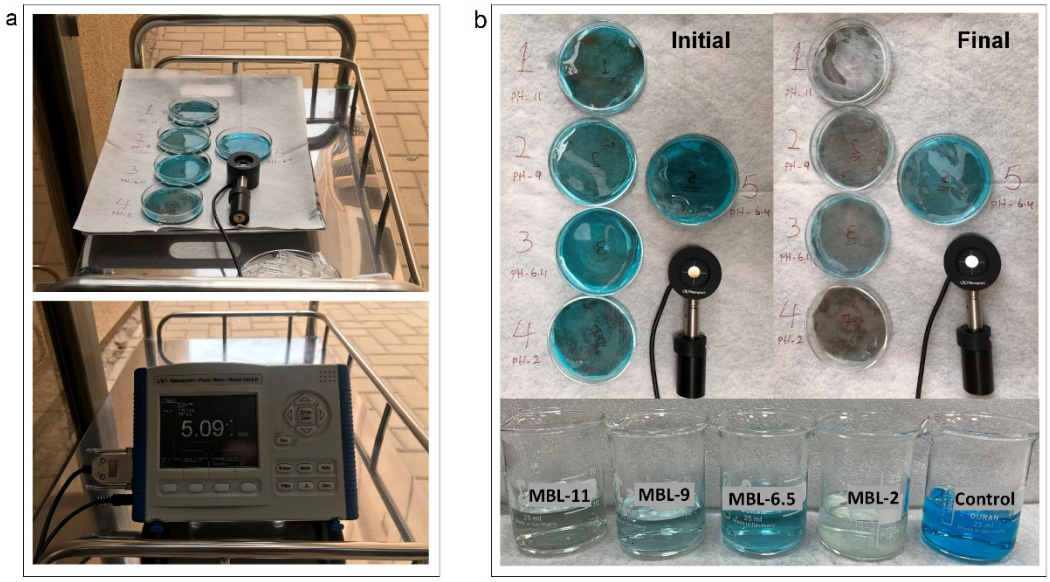

Figure S3. Photographs of (a) the experiments setup with the photodetector and samples exposed to natural sunlight in a shaded area and (b) the initial and final visualized color of the MB dyes on the disks and their final degraded dyes in the beakers

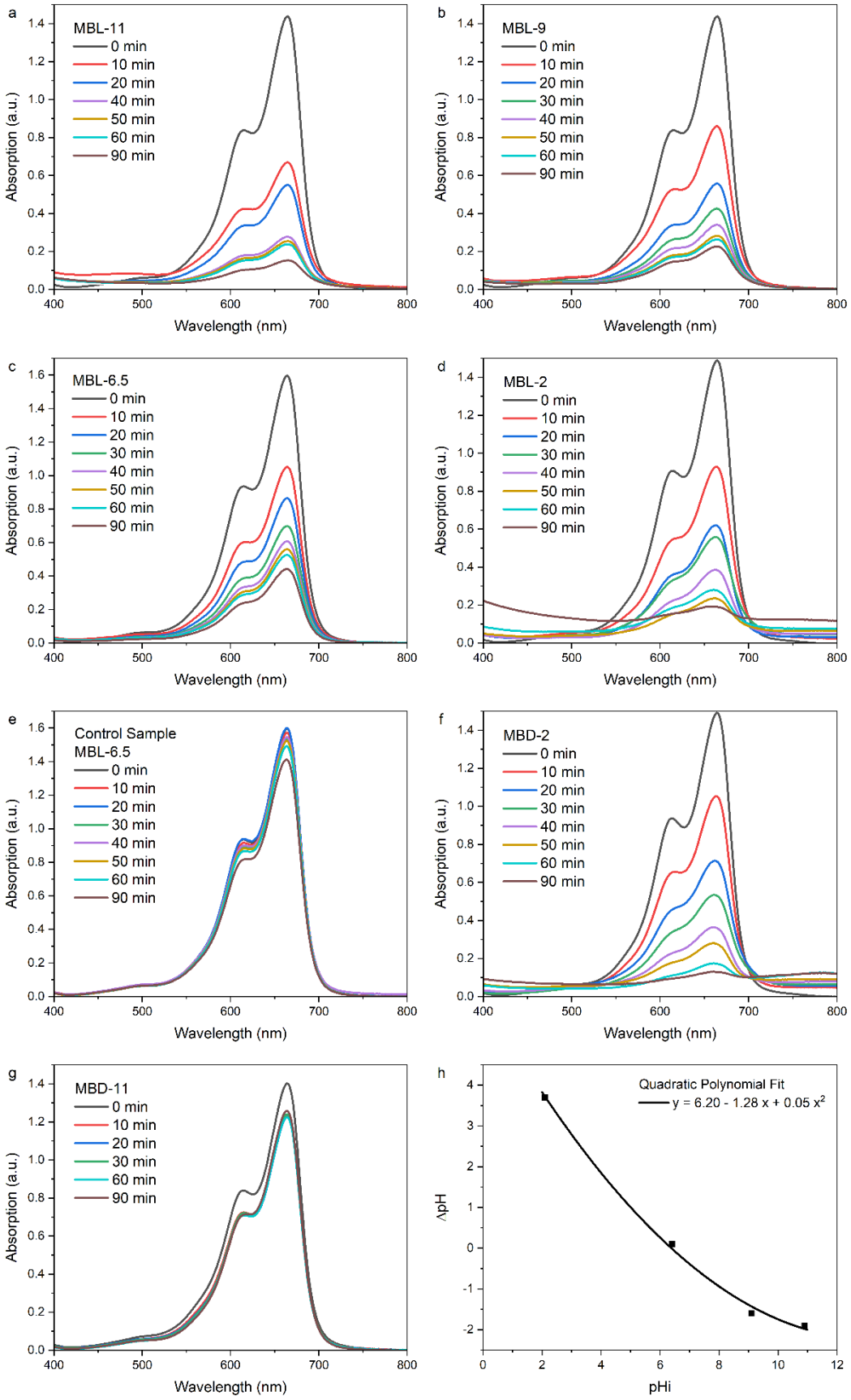

Figure S4. (a-g) UV-Vis absorption spectra of MBL-11, MBL-9, MBL-6.5, MBL-2, control sample MBL-6.5, MBD-2, and MBD-11, respectively, during 90 minutes and (h) the change between the final and initial pH values (ΔpH) for all these samples

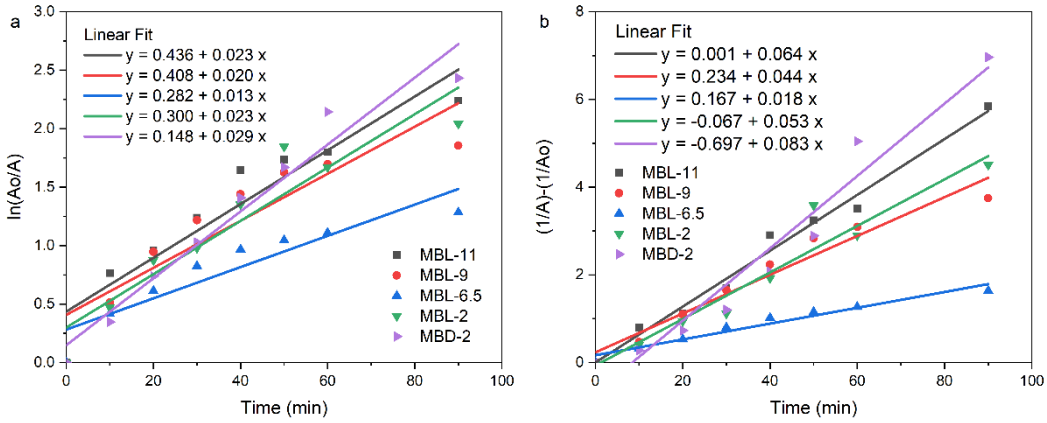

Figure S5. The linear fitting of the MB experimental data with (a) the first-order kinetic model, and (b) the second-order kinetic model

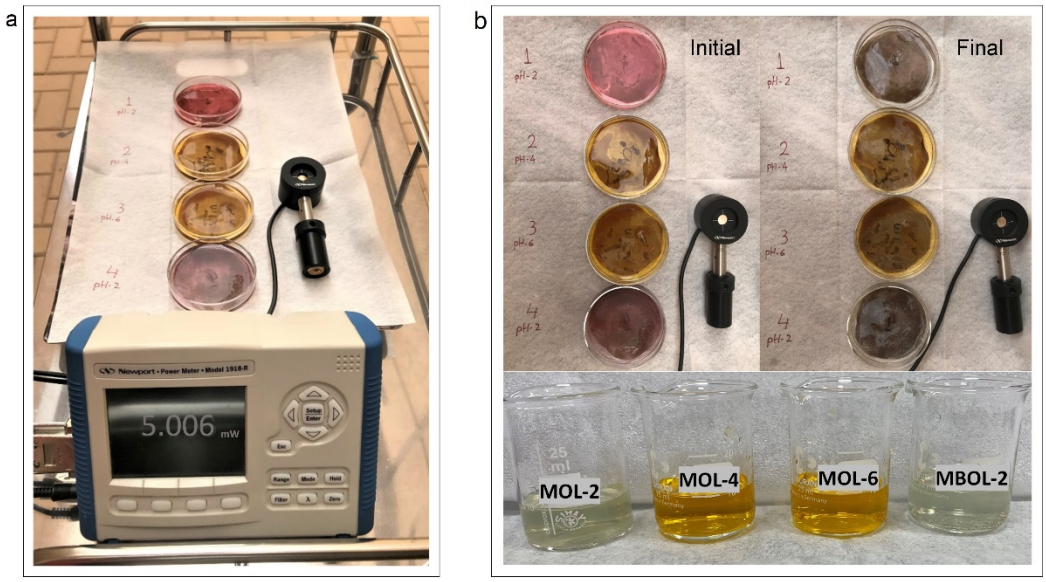

Figure S6. Photographs of (a) the experiments setup with the photodetector and samples exposed to natural sunlight in a shaded area and (b) the initial and final visualized color of the MO and MB/MO dyes on the disks and their final degraded dyes in the beakers

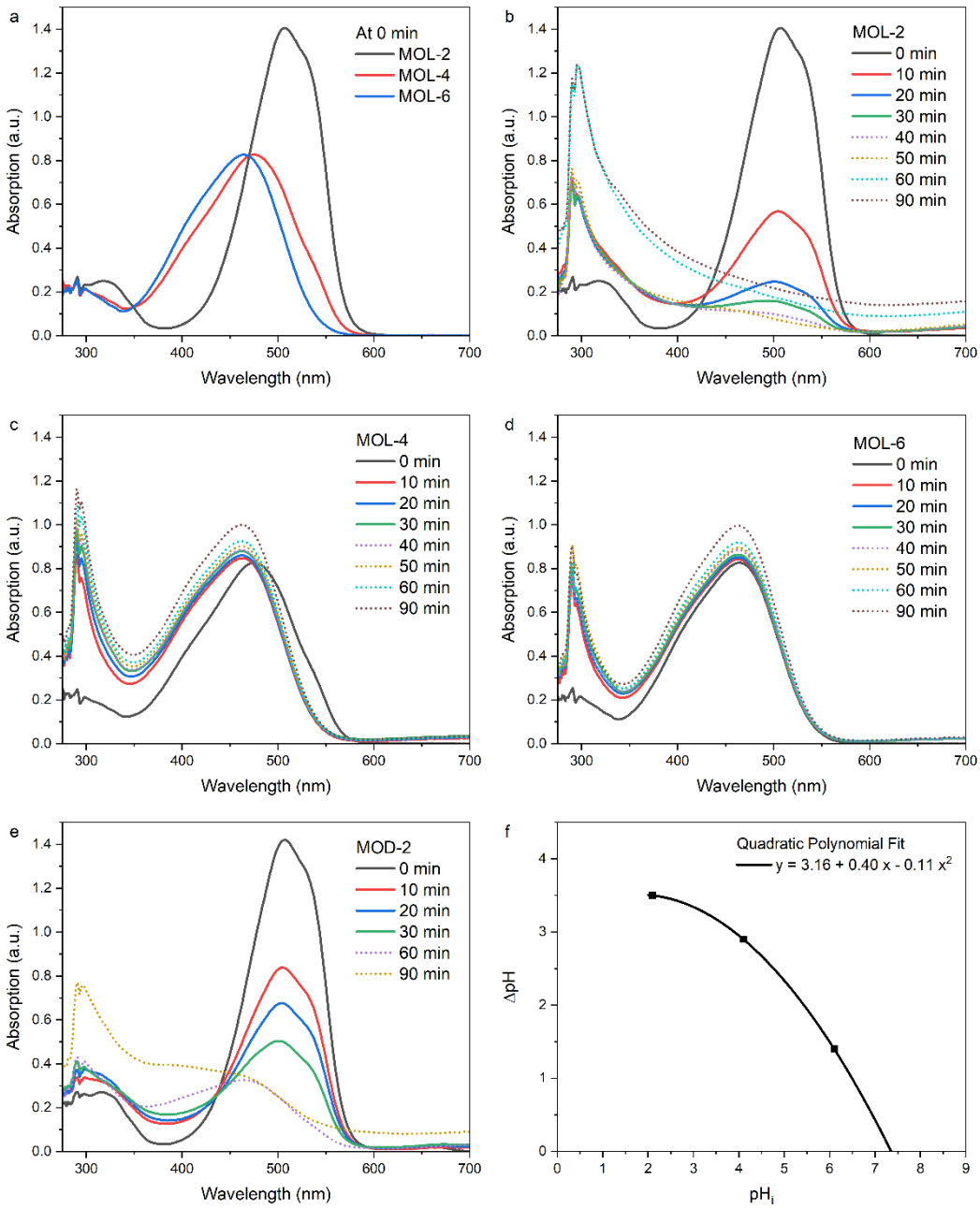

Figure S7. (a) UV-Vis absorption spectra at initial pH values and (b-e) UV-Vis absorption spectra of MOL-2, MOL-4, MOL-6, and MOD-2, respectively, during 90 minutes and (f) the change between the final and initial pH values (ΔpH) for all these samples

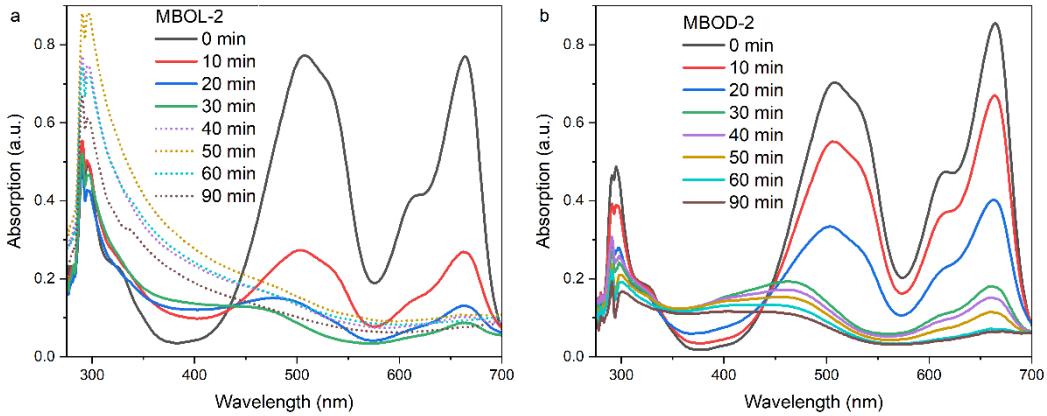

Figure S8. (a and b) UV-Vis absorption spectra of MBOL-2 and MBOD-2, respectively, during 90 minutes.